Electronic Supplementary Material (ESI) for ChemComm.
This journal is © The Royal Society of Chemistry 2020

Electronic Supporting Information

$Ba(B_2OF_3(OH)_2)_2$ with well-ordered OH/F anions constructing a unique $B_2OF_3(OH)_3$ dimer

Minqiang Gai,[a,b,†] Ying Wang,[a,†] Tinghao Tong,[a,b] Liying Wang,[c] Zhihua Yang,[a] Xin Zhou,[c] and Shilie Pan*,[a]

[a]CAS Key Laboratory of Functional Materials and Devices for Special Environment, Xinjiang Technical Institute of Physics & Chemistry, CAS; Xinjiang Key Laboratory of Electronic Information Materials and Devices, 40-10 South Beijing Road, Urumqi 830011, China

[b]Center of Materials Science and Optoelectronics Engineering, University of Chinese Academy of Sciences, Beijing 100049, China

[c]Key Laboratory of Magnetic Resonance in Biological Systems, State Key Laboratory of Magnetic Resonance and Atomic and Molecular Physics, National Center for Magnetic Resonance in Wuhan, Wuhan Institute of Physics and Mathematics, CAS, Wuhan 430071, China

[†]These authors contributed equally to this work.

E-mail address: slpan@ms.xjb.ac.cn.

Table of Contents

Experimental Section

Synthetic Procedure. All starting materials, $BaCO_3$ (AR, 99.9 %), H_3BO_3 (AR, 99.0 %, Aladdin), distilled water and fluoroboric acid (40 %, Aladdin) were commercially available and used as received. $Ba(B_2OF_3(OH)_2)_2$ (BBOFH) can be obtained by hydrothermal method based on the following reaction: $2BaCO_3 + 3HBF_4 + 5H_3BO_3 = 2Ba(B_2OF_3(OH)_2)_2 + 2CO_2\uparrow + 5H_2O$. The molar ratio of $BaCO_3$ and HBO_3 was 2 : 5, respectively. Then, a mixture of 0.25 mL of HBF_4 and 1 ml distilled water were added. HBF_4 serves as both a fluorine source and a mineralizer. The resultant opaque, colorless slurry was stirred mechanically for 3 min, then placed in a 50 mL capacity Teflon-lined Parr autoclave and heated statically at 220 °C for 3 days. The product was recovered by suction filtration and washed with alcohol, with a typical yield of 61.8% based on Ba and 12 × 4 × 3 mm^3 crystals of BBOFH were obtained. We have also carried on the wet chemical analysis of BBOFH. The experimental route is as follows: First, the BBOFH samples were placed in a plastic pipe; Second, hydrochloric acid was continuously dripped into the pipe; No bubbles were observed in the course of the experiment, showing that there is no chemical reaction and no CO_3 existed in the compound. This indicates that there is no incorporation of carbonate ions in the product. As for fluorooxoborates, we should point out that the crystal growth of fluorooxoborates with large sizes is still a great challenge, which is of great importance for practical applications. Because fluorooxoborates are often not congruent melting compounds and their weak thermal stability, the solvothermal method and hydrothermal method might be better approaches for large single crystals growth.

Characterization Methods. Crystals ground into powder were characterized by powder X-ray diffraction (XRD) on a Bruker D2 PHASER diffractometer with Cu Kα radiation (λ=1.5418 Å) at room temperature, scan range of 10 to 70° (2θ). The fixed counting time and scan step width are 1s/step and 0.02°, respectively. All samples were ground thoroughly in a mortar and pestle before mounting the resultant powder in the sample holder. A full Rietveld refinement has been performed by using the GSAS II (Figure S1). The R_p value is 6.99 %, indicating the reasonable degree of agreement between experimental XRD patterns and the theoretical ones except for one little impurity peak at about 22°.

A Bruker SMART APEX II 4K CCD diffractometer with Mo Kα radiation (λ=0.71073 Å) was used to collect the single-crystal XRD data at 153 K. And the data were integrated with the SAINT program. The direct methods and the Olex2 program[1] were used to solve and refine the crystal structure, respectively. All of the atoms' positions were refined by full matrix least-squares techniques. The H positions were located in the difference Fourier maps with displacement parameters assigned as Uiso(H) = 1.2Ueq(O). The information of crystal data and structural refinement is summarized in Table 1. The selected bond lengths and angles are listed in Tables S3 and S4. The anisotropic displacement parameters (A^2 x 10^3) (Table S5), hydrogen bonds (Table S6), Hydrogen coordinates (x 10^4) and isotropic displacement parameters (A^2 x 10^3) (Table S7) for BaBOFH are also listed.

Thermal gravimetric (TG) analyses were carried out on a NETZSCH STA 449F3 thermal analyzer instrument in the temperature range 40-1000 ℃ with a heating rate of 5 ℃min^{-1} in an atmosphere of flowing N_2. UV/Vis/NIR transmission data of BBOFH was collected on a Shimadzu SolidSpec-3700DUV spectrophotometer over the 180–2600 nm spectral range, at room temperature. Crystals ground into a powder were characterized by solid state Nuclear Magnetic Resonance (NMR), which was carried out with a Bruker Avance III 500 WB (11.75 T) spectrometer operating at a frequency of 470.96 and 160.61 MHz for ^{19}F and ^{11}B, respectively. A commercial DVT quadruple resonance H/F/X/Y 2.5 mm CP/MAS probe was used with a spinning frequency of 30.0 kHz. Solid-state ^{19}F MAS NMR spectra were recorded with a single pulse excitation using a 90 degree pulse width of 1.9 us (pi/2) and a recycle delay of 5 s to obtain quantitative results. There is no fluorine background from the H/F/X/Y probehead. ^{19}F chemical shifts were determined using a solid external reference, Poly (tetrafluoroethylene) (PTFE). The CF2 groups of PTFE resonate at -122 ppm relative to tetramethylsilane (TMS). ^{11}B MAS NMR spectra was recorded, with a single pulse excitation using a short pulse length (0.32 us) to obtain quantitative results, and a recycle delay of 10 s (the tip angle was pi/12). ^{11}B chemical shifts were referenced using H_3BO_3 1 M in solution as an external reference (19.6 ppm). The presence of B-F bonds was checked employing $^{11}B\{^{19}F\}$-REDOR NMR spectroscopy, which enables the determination of the heteronuclear ^{11}B-^{19}F dipole coupling and hence the evaluation of internuclear distances. Solid-state ^{1}H MAS NMR spectra were recorded with a single pulse excitation, a 90° pulse length of 3.4 μs and a recycle delay of 4 s were applied to obtain quantitative results.

Energy dispersive X-ray spectroscope (EDX) was carried on clean single crystal surface with the aid of a field emission scanning electron microscope equipped with an X-Max^N (Oxford Instruments) energy-dispersive spectrometer.

IR spectra of BBOFH were performed on the KBr matrixes in the 400–4000 cm^{-1} range using a Shimadzu IR Affinity-1 Fourier transform infrared spectrometer, at room temperature, with a resolution of 2 cm^{-1}. 6 mg of sample was mixed thoroughly with 500 mg of dried KBr.

The microstructure of the BBOFH samples was observed by X-ray photoelectron spectroscopy (XPS) performed on an ESCALAB 250Xi electron spectrometer (Thermo Fisher Scientific) with Al Kα radiation. As expected, a full survey of BBOFH reveals the presence of four elements, namely, Ba, B, F, and O (Figure S12). The XPS analysis indicates that the atomic molar ratio of Ba : B : O : F is 1 : 3.71 : 6.36 : 5.95 (Table S9), which is approximately equal to the theoretical ratio of 1 : 4 : 6 : 6, further verifying the validity of the structure model.

Neutron powder diffraction (NPD) experiments were performed on the time-of-flight diffractometer GPPD (the general purpose powder diffractometer) at CSNS (the China Spallation Neutron Source), Dongguan, China. The sample is loaded in 9-mm vanadium can and the pattern is collected with wavelength bands of 0.1 - 4.9 Å. The NPD pattern is refined by the Rietveld method using the general structure analysis system (GSAS) suite of programs.[31]

Computational Methods. The electronic structures of BBOFH was calculated using the density functional theory method embedded in the CASTEP package.[2] The exchange-correlation functional was the Perdew-Burke-Emzerhof (PBE) functional within the generalized gradient approximation (GGA).[3] The plane wave cut-off energy was set at 940 eV. Self consistent-field calculations were performed with a convergence criterion of 5 × 10^{-7} eV/atom on the total energy. The

k-point separation for each material was set as 0.05 $Å^{-1}$ in the Brillouin zone. PWmat code[4] was adopted to obtain more accurate bandgap of BBOFH. First-principles calculations based on density functional theory (DFT) with local density approximation (LDA) were performed by a plane-wave pseudopotential calculation package CASTEP. We calculated the phonon spectra of BBOFH and artificial compounds by mutual substitution of the F atoms and the hydroxy linked with the B atoms. The calculated phonon spectrum of the artificial structure of $Ba[B_2OF_5]_2$ was failed because of the structural instability.

Table S1. Crystal data and structure refinement for BBOFH

Empirical formula	$Ba(B_2OF_3(OH)_2)_2$
Formula weight (g/mol)	394.61
Temperature (K)	153
Crystal system	Monoclinic
Space group	*C2/m*
a (Å)	6.803(2)
b (Å)	7.008(2)
c (Å)	9.588(3)
β (deg)	92.960(4)
Volume (Å^3)	456.5(3)
Z	2
Absorption coefficient (mm^{-1})	4.461
F (000)	364
θ range for data collection (°)	4.178 to 27.524
Reflections collected / unique	1398 / 565 [*R(int)* = 0.0179]
Completeness (%)	99.3
Data / restraints / parameters	565/0/54
GOF on F^2	1.097
Final *R* indices [$F > 2\sigma(F)$]^a	R_1 = 0.0144, wR_2 =0.0324
R indices (all data)^a	R_1= 0.0144, wR_2 = 0.0324

$^aR_1 = \Sigma||F_o| - |F_c||/\Sigma|F_o|$ and $wR_2 = [\Sigma w(F_o^2 - F_c^2)^2/\Sigma wF_o^4]^{1/2}$ for $F_o^2 > 2\sigma(F_o^2)$.

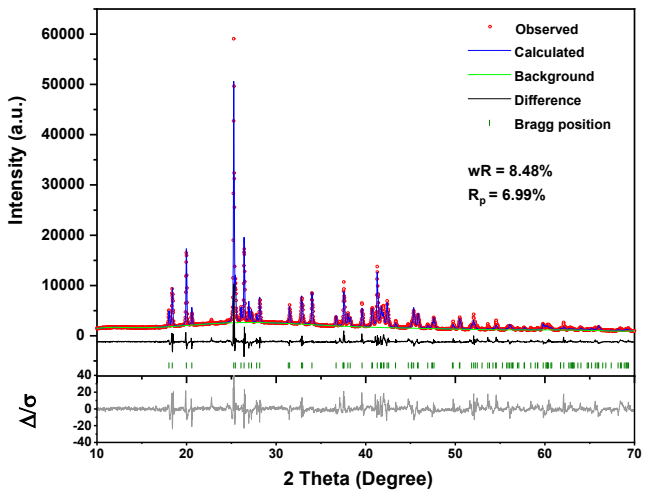

Figure S1. Rietveld refined XRD patterns of BBOFH.

Table S2. Atomic coordinates and equivalent isotropic displacement parameters and bond valence sum (BVS) calculation for BBOFH. U(eq) is defined as one third of the trace of the orthogonalized U_{ij} tensor.

Atom	x	y	z	U(eq)	BVS[5]
Ba1	½	1	1	0.0083(9)	2.089
B1	0.7584(5)	½	0.6154(3)	0.0153(7)	3.029
B2	0.5430(5)	½	0.8158(3)	0.0107(6)	3.132
O1	0.7721(3)	½	0.4743(2)	0.0258(6)	1.873
O2	0.9262(3)	½	0.7016(2)	0.0185(5)	2.087
O3	0.5773(3)	½	0.6710(19)	0.0135(4)	1.885
F1	0.6310(17)	0.66148(16)	0.8854(12)	0.0139(2)	1.068
F2	0.3420(2)	½	0.8347(16)	0.0141(3)	0.964

Table S3. Bond distances (Å) for BBOFH.

Atom	Atom	Length/Å	Atom	Atom	Length/Å
Ba1	O2^{1}	2.879(2)	Ba1	F2^{8}	2.8819(19)
Ba1	O2^{2}	2.879(2)	Ba1	F2^{9}	2.8819(19)
Ba1	F1	2.7803(13)	B1	O1	1.361(4)
Ba1	F1^{3}	2.9161(14)	B1	O2	1.374(4)
Ba1	F1^{4}	2.7802(13)	B1	O3	1.367(4)
Ba1	F1^{5}	2.7802(13)	B2	O3	1.421(4)
Ba1	F1^{1}	2.9161(14)	B2	F1	1.429(2)
Ba1	F1^{2}	2.9161(14)	B2	F1^{10}	1.429(2)
Ba1	F1^{6}	2.7802(13)	B2	F2	1.388(4)
Ba1	F1^{7}	2.9161(14)			

^{1}3/2-X,3/2-Y,2-Z; ^{2}-1/2+X,1/2+Y,+Z; ^{3}3/2-X,1/2+Y,2-Z; ^{4}1-X,2-Y,2-Z; ^{5}+X,2-Y,+Z; ^{6}1-X,+Y,2-Z; ^{7}-1/2+X,3/2-Y,+Z; ^{8}1/2+X,1/2+Y,+Z; ^{9}1/2-X,3/2-Y,2-Z; ^{10}+X,1-Y,+Z

Table S4. Bond angles (deg) for BBOFH.

Atom	Atom	Atom	Angle/°	Atom	Atom	Atom	Angle/°
O2^{1}	Ba1	O2^{2}	180.0	F1	Ba1	F1^{4}	101.11(3)
O2^{1}	Ba1	F1^{3}	61.52(5)	F1^{9}	Ba1	F1^{3}	101.11(3)
O2^{1}	Ba1	F1^{2}	118.48(5)	F1^{8}	Ba1	F1^{4}	62.00(4)
O2^{2}	Ba1	F1^{1}	118.48(5)	F1^{9}	Ba1	F1	180.0
O2^{2}	Ba1	F1^{4}	61.52(5)	F1	Ba1	F1^{3}	78.89(3)
O2^{1}	Ba1	F1^{4}	118.48(5)	F1^{8}	Ba1	F1^{7}	180.0
O2^{1}	Ba1	F1^{1}	61.52(5)	F1^{9}	Ba1	F1^{8}	62.86(5)
O2^{2}	Ba1	F1^{2}	61.52(5)	F1^{8}	Ba1	F1^{1}	78.89(3)
O2^{2}	Ba1	F1^{3}	118.48(5)	F1^{9}	Ba1	F2^{5}	59.89(3)
O2^{2}	Ba1	F2^{5}	63.76(6)	F1^{7}	Ba1	F2^{5}	59.89(3)
O2^{2}	Ba1	F2^{6}	116.24(6)	F1^{7}	Ba1	F2^{6}	120.11(3)

O2[1]	Ba1	F2[6]	63.76(6)	F1[9]	Ba1	F2[6]	120.11(3)
O2[1]	Ba1	F2[5]	116.24(6)	F1[8]	Ba1	F2[6]	59.89(3)
F1	Ba1	O2[2]	110.47(3)	F1[8]	Ba1	F2[5]	120.11(3)
F1[7]	Ba1	O2[2]	69.53(3)	F1	Ba1	F2[6]	59.89(3)
F1[8]	Ba1	O2[2]	110.47(3)	F1	Ba1	F2[5]	120.11(3)
F1	Ba1	O2[1]	69.53(3)	F2[6]	Ba1	F1[2]	60.23(4)
F1[9]	Ba1	O2[2]	69.53(3)	F2[6]	Ba1	F1[4]	60.23(4)
F1[8]	Ba1	O2[1]	69.53(3)	F2[6]	Ba1	F1[1]	119.77(4)
F1[7]	Ba1	O2[1]	110.47(3)	F2[5]	Ba1	F1[3]	60.23(4)
F1[9]	Ba1	O2[1]	110.47(3)	F2[5]	Ba1	F1[1]	60.23(4)
F1[9]	Ba1	F1[2]	118.00(4)	F2[5]	Ba1	F1[2]	119.77(4)
F1[3]	Ba1	F1[2]	134.33(5)	F2[5]	Ba1	F1[4]	119.77(4)
F1	Ba1	F1[2]	62.00(4)	F2[6]	Ba1	F1[3]	119.77(4)
F1[4]	Ba1	F1[2]	45.67(5)	F2[5]	Ba1	F2[6]	180.0
F1[8]	Ba1	F1[3]	118.00(4)	O1	B1	O2	120.0(3)
F1[7]	Ba1	F1[2]	78.89(3)	O1	B1	O3	119.8(2)
F1[9]	Ba1	F1[7]	117.14(5)	O3	B1	O2	120.2(3)
F1[7]	Ba1	F1	62.86(5)	O3	B2	F1	111.73(17)
F1[9]	Ba1	F1[4]	78.89(3)	O3	B2	F1[10]	111.73(16)
F1[2]	Ba1	F1[1]	180.0	F1	B2	F1[10]	104.7(2)
F1[7]	Ba1	F1[3]	62.00(4)	F2	B2	O3	109.9(2)
F1[8]	Ba1	F1[2]	101.11(3)	F2	B2	F1	109.32(17)
F1[8]	Ba1	F1	117.14(5)	F2	B2	F1[10]	109.32(17)
F1[3]	Ba1	F1[1]	45.67(5)				
F1[7]	Ba1	F1[4]	118.00(4)				
F1[4]	Ba1	F1[1]	134.33(5)				
F1[9]	Ba1	F1[1]	62.00(4)				
F1[7]	Ba1	F1[1]	101.11(3)				
F1	Ba1	F1[1]	118.00(4)				
F1[4]	Ba1	F1[3]	180.0				

Symmetry transformations used to generate equivalent atoms:

[1]-1/2+X,1/2+Y,+Z; [2]3/2-X,3/2-Y,2-Z; [3]-1/2+X,3/2-Y,+Z; [4]3/2-X,1/2+Y,2-Z; [5]1/2-X,3/2-Y,2-Z; [6]1/2+X,1/2+Y,+Z; [7]1-X,+Y,2-Z; [8]+X,2-Y,+Z; [9]1-X,2-Y,2-Z; [10]+X,1-Y,+Z; [11]1/2+X,-1/2+Y,+Z; [12]-1/2+X,-1/2+Y,+Z

Table S5. Anisotropic displacement parameters ($A^2 \times 10^3$) for BBOFH. The anisotropic displacement factor exponent takes the form:

$$-2\pi^2 [h^2 a^{*2} U_{11} + ... + 2 h k a^* b^* U_{12}]$$

Atom	U_{11}	U_{22}	U_{33}	U_{23}	U_{13}	U_{12}
Ba1	5.85(12)	10.64(13)	8.38(12)	0	0.29(8)	0
B1	11.2(15)	23.7(17)	11.1(14)	0	2.5(12)	0
B2	6.7(14)	15.6(15)	9.9(14)	0	1.2(11)	0

O1	8.0(11)	59.4(17)	9.8(10)	0	-0.7(8)	0
O2	8.2(10)	39.0(13)	8.3(9)	0	1.2(8)	0
O3	7.6(9)	24.6(11)	8.2(9)	0	0.3(7)	0
F1	13.2(6)	14.5(6)	14.0(5)	-2.4(5)	0.7(5)	-0.9(5)
F2	7.6(8)	22.9(9)	12.1(8)	0	3.6(6)	0

Table S6. Hydrogen bonds for BBOFH.

D	H	A	d(D-H)/Å	d(H-A)/Å	d(D-A)/Å	D-H-A/°
O1	H1	O3[1]	0.87(4)	1.83(4)	2.692(3)	176(4)
O1	H1	F2[1]	0.87(4)	2.55(4)	3.024(3)	115(3)
O2	H2	O1[2]	0.85(4)	1.89(4)	2.722(3)	168(3)

[1]1-X,1-Y,1-Z; [2]2-X,1-Y,1-Z

Table S7. Hydrogen coordinates (x 10^4) and isotropic displacement parameters ($A^2 \times 10^3$) for BBOFH.

Atom	x	y	z	U(eq)
H1	6570(60)	5000	4310(40)	31
H2	10310(60)	5000	6580(40)	22

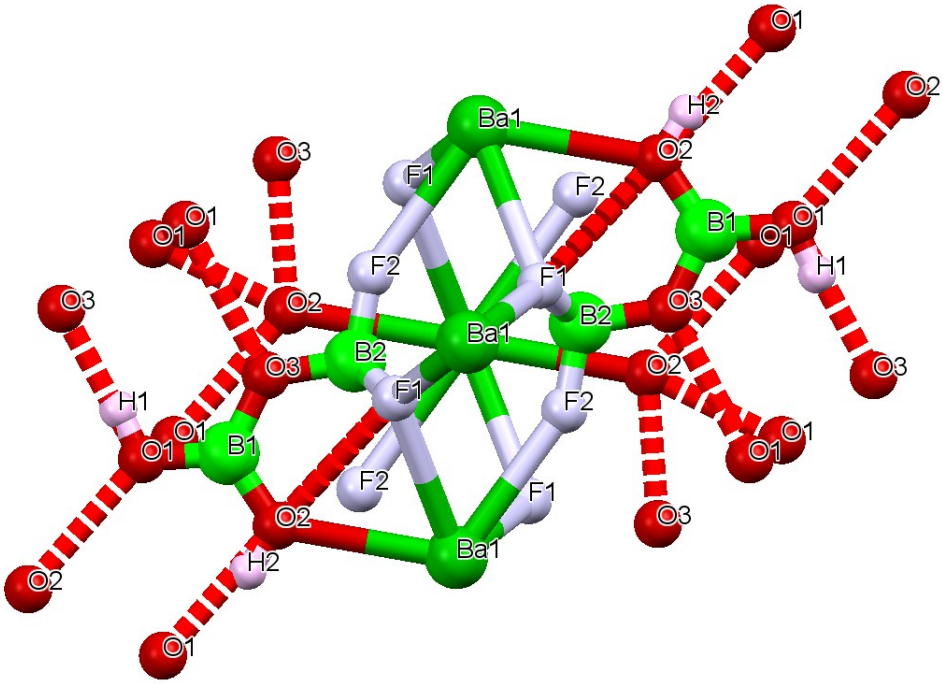

Figure S2. Asymmetric units of BBOFH. The dotted red line denotes the hydrogen bonding H • • • O

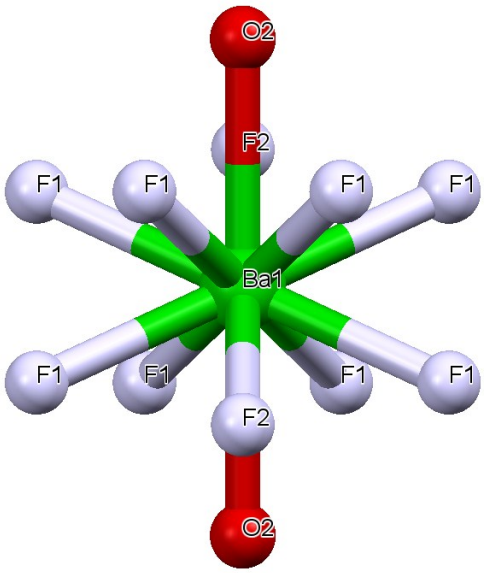

Figure S3. Coordination environments of cations in BBOFH.

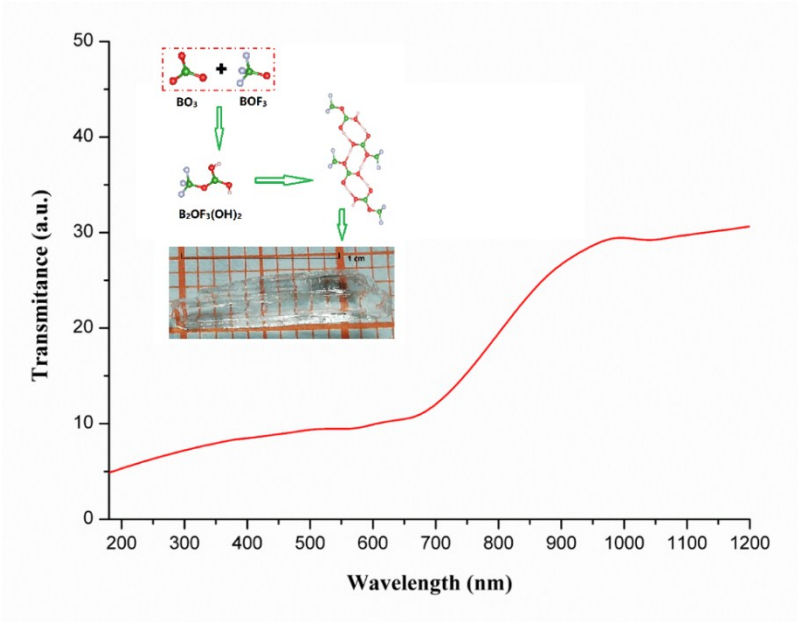

Figure S4. The ultraviolet-visible-near-infrared transmittance spectrum of BBOFH.

Table S8. The investigation of anionic units in the inorganic fluorooxoborates.

BO_3F	BO_2F_2	BOF_3
LiB_6O_9F[6]	$Li_2B_6O_9F_2$[7]	BBOFH
$Li_2B_3O_4F_3$[8]	$Li_2B_3O_4F_3$[8]	
NaB_4O_6F[9]	$Na_3B_3O_3F_6$[10]	
$NH_4B_4O_6F$[11]	$Na_2B_6O_9F_2$[12]	
RbB_4O_6F[13]	$K_3B_3O_3F_6$[14]	
$K_3B_6O_9F_3$[15]	$K_3B_6O_9F_3$[15]	
CsB_4O_6F[16]	$NaRbB_6O_9F_2$[17]	
$CsKB_8O_{12}F_2$[13]	$BaBOF_3$[18]	
$CsRbB_8O_{12}F_2$[13]	$Na_3B_7O_{11}F_2$[19]	
$Li_2Na_{0.9}K_{0.1}B_5O_8F_2$[20]	$K_{0.42}Rb_{2.58}B_3O_3F_6$[21]	
$CaB_4O_6F_2$[22]		
$CaB_5O_7F_3$[23]		
$SrB_4O_6F_2$[22]		
$SrB_5O_7F_3$[24]		
$BaB_4O_6F_2$[25]		
$SnB_2O_3F_2$[26]		
$PbB_2O_3F_2$[26]		
PbB_5O_8F[27]		
BiB_2O_4F[28]		
$BaB_2O_3F_2$[29]		
$BaB_8O_{12}F_2$[30]		

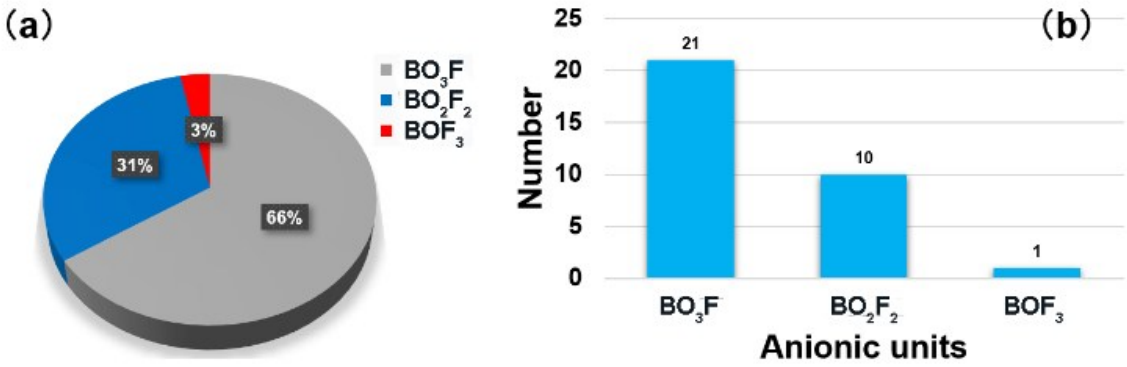

Figure S5. (a) Compounds proportion and (b) distribution of anionic units in inorganic fluorooxoborates.

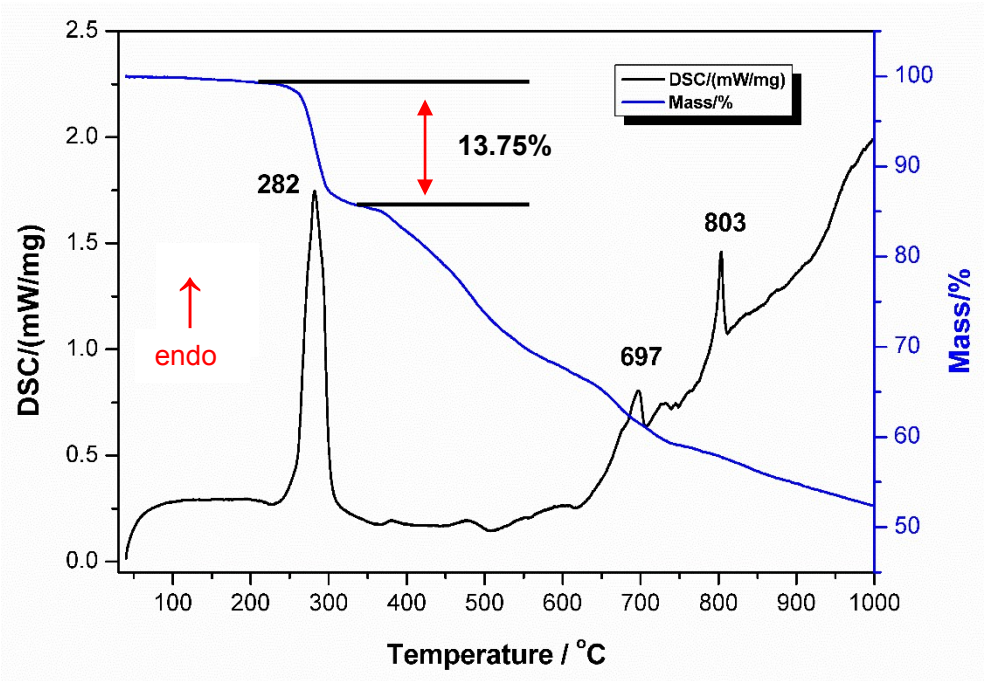

Figure S6. TG and DSC curves of BBOFH in the temperature region 40–1000 °C. It is speculated that the decomposition of BBOFH follows the following equation: $Ba(B_2OF_3(OH)_2)_2 = BaB_2O_4 + 2H_2O + 2BF_3\uparrow$. The calculated weight loss of H_2O and gas is about 43.5 %, which is close to experimental one.

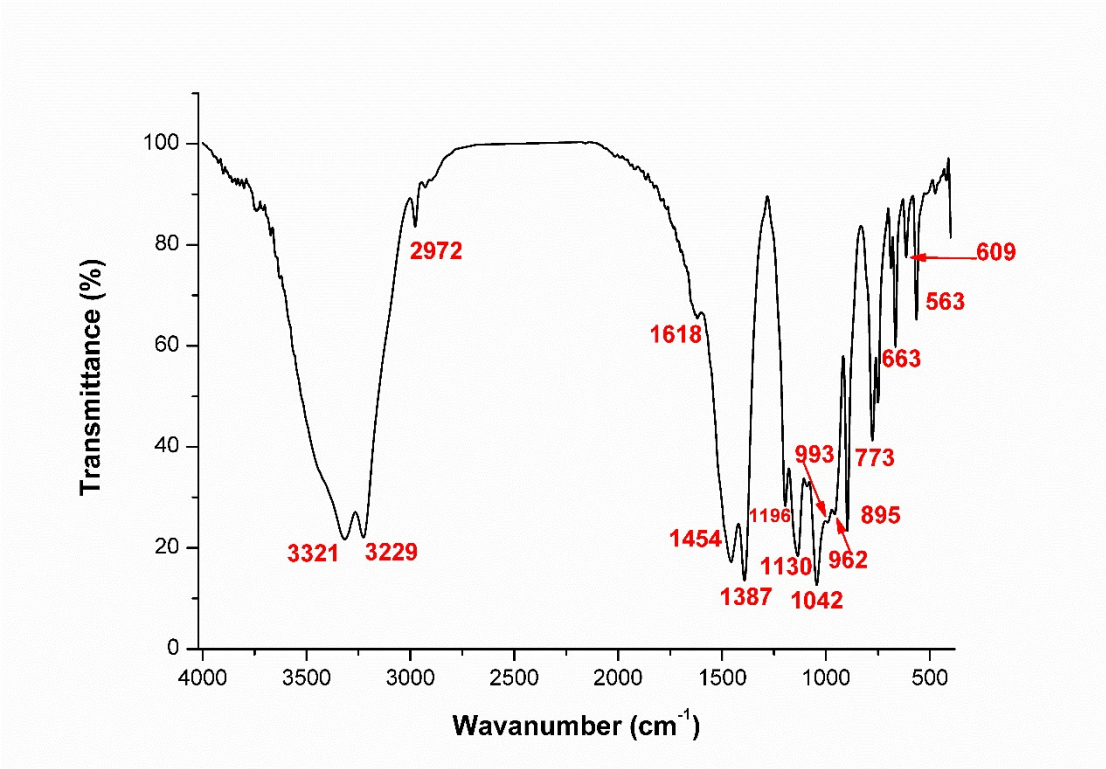

Figure S7. The infrared spectrum of BBOFH.

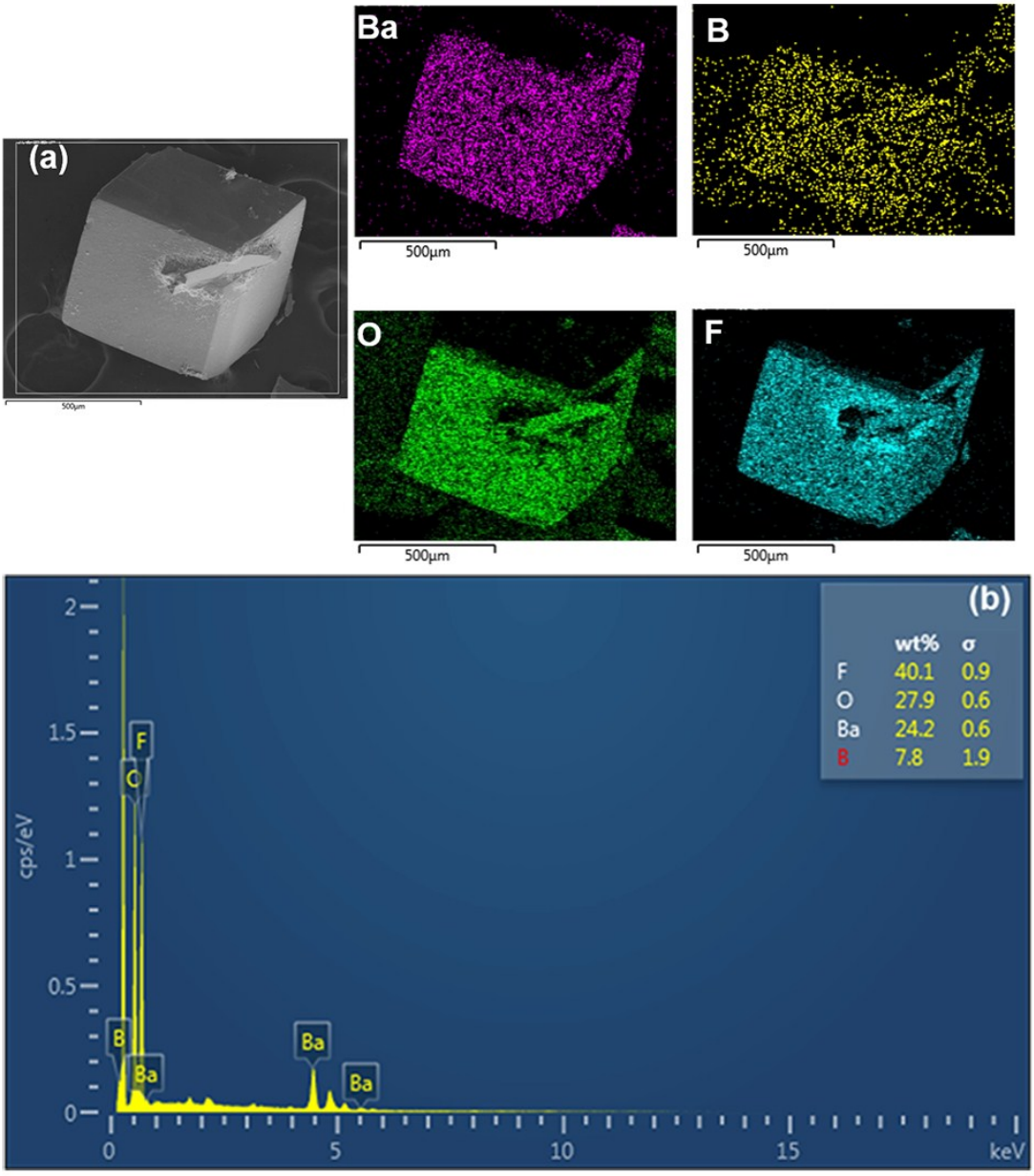

Figure S8. (a) SEM image of BBOFH and its elemental distribution maps, (b) Energy-dispersive X-ray spectroscopy of BBOFH.

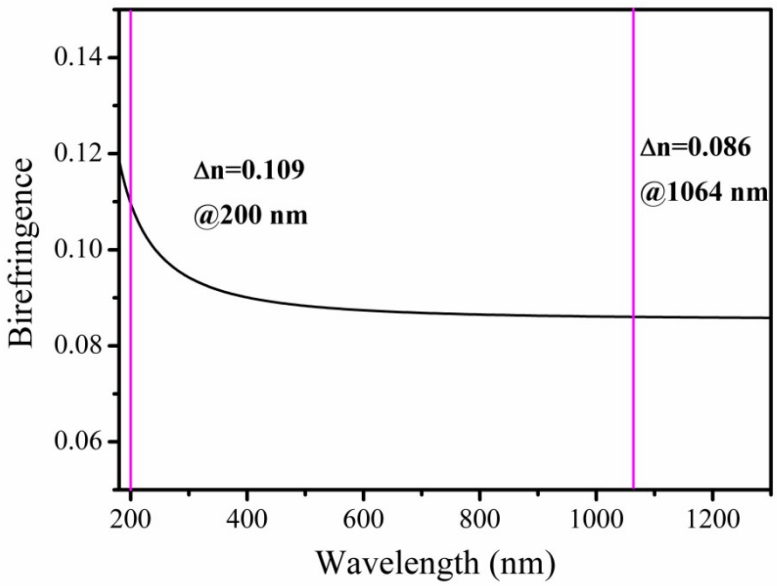

Figure S9. Calculated birefringence curve of BBOFH.

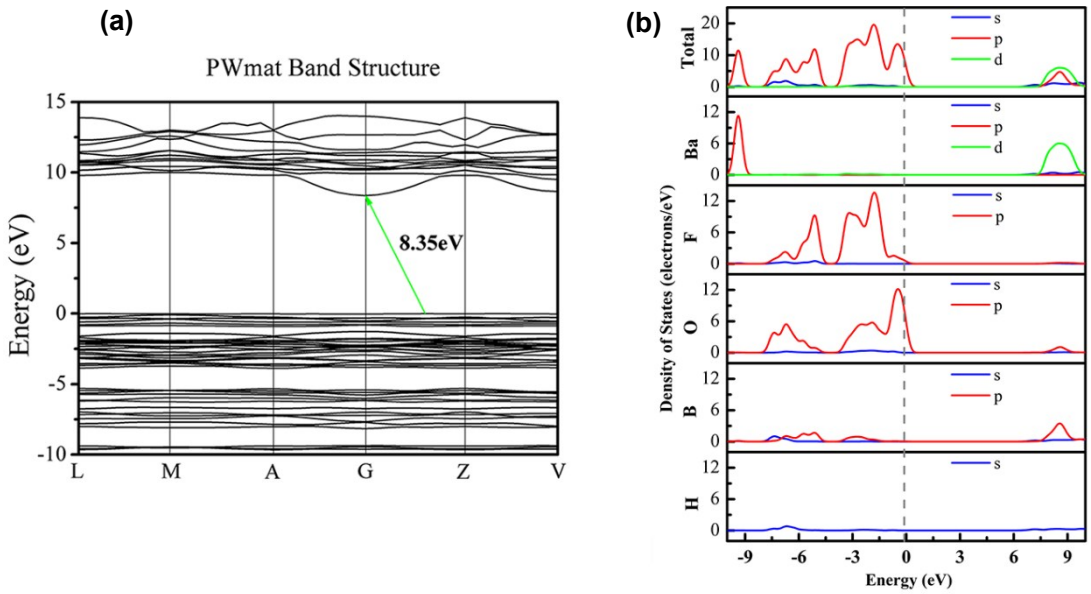

Figure S10. Band structure and total and partial density of states for BBOFH (a, b).

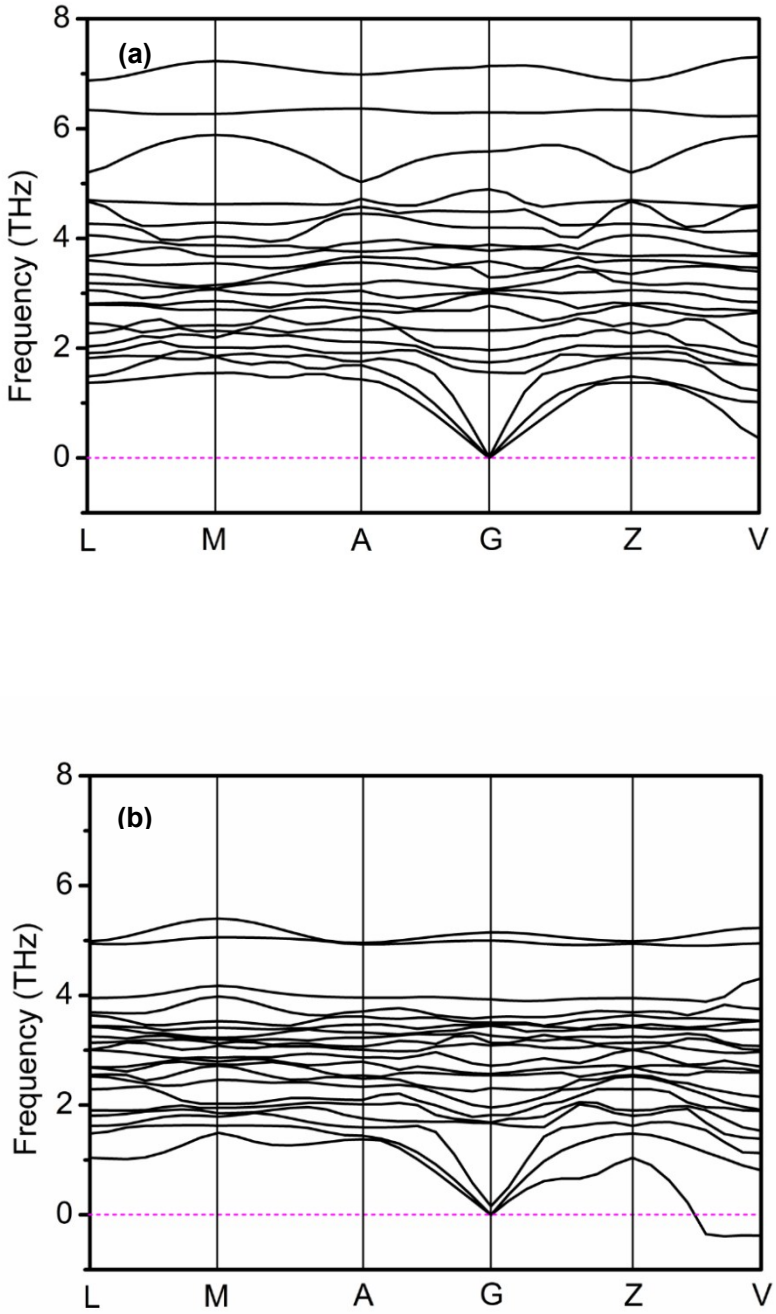

Figure S11. Phonon spectrum of BBOFH (a)，and artificial structure of BBOFH with partially replaced hydroxyl group by the F atoms (b).

(b)

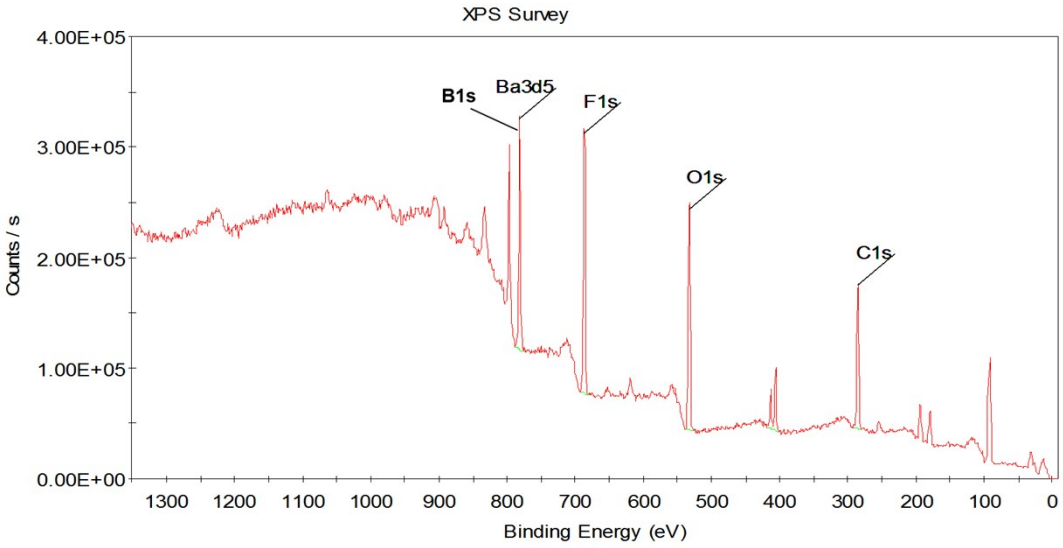

Figure S12. XPS full spectra of BBOFH.

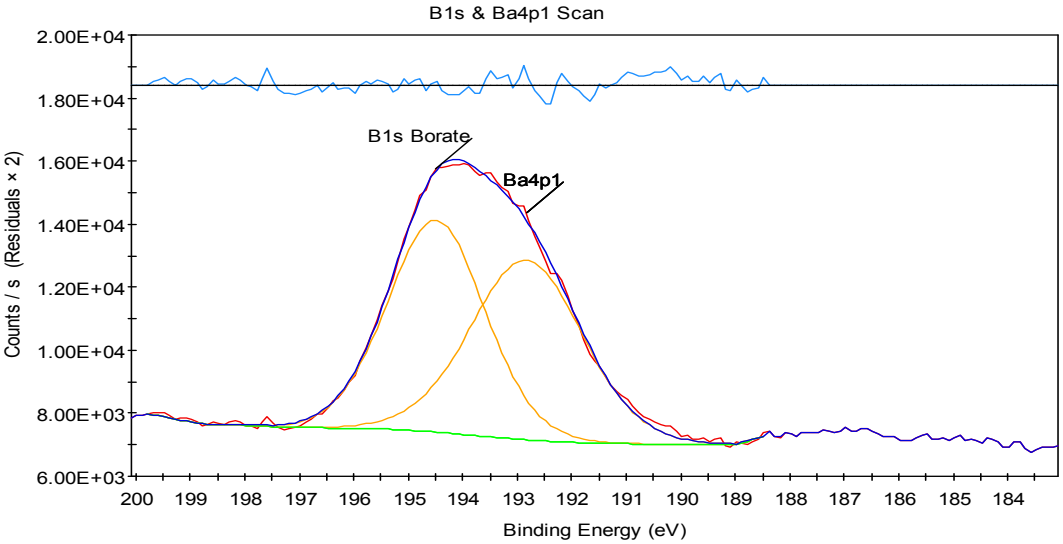

Figure S13. XPS full spectra of B1s and Ba4p1.

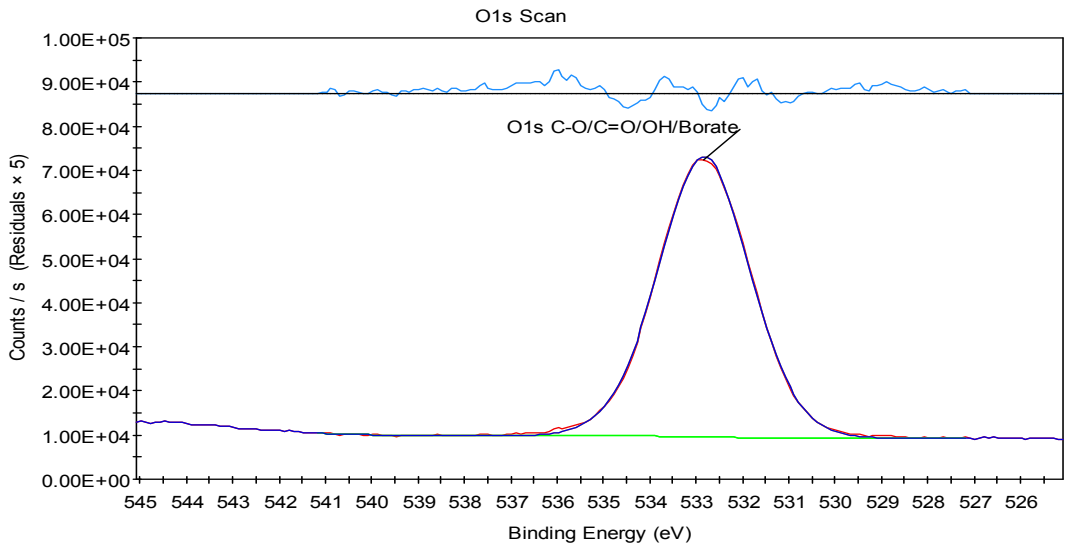

Figure S14. XPS full spectra of O1s.

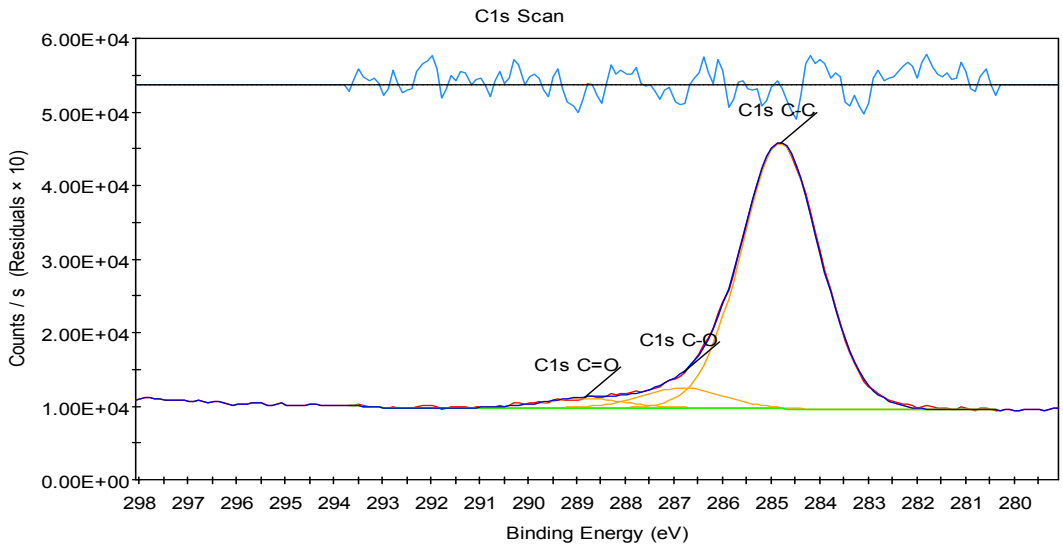

Figure S15. XPS full spectra of C1s.

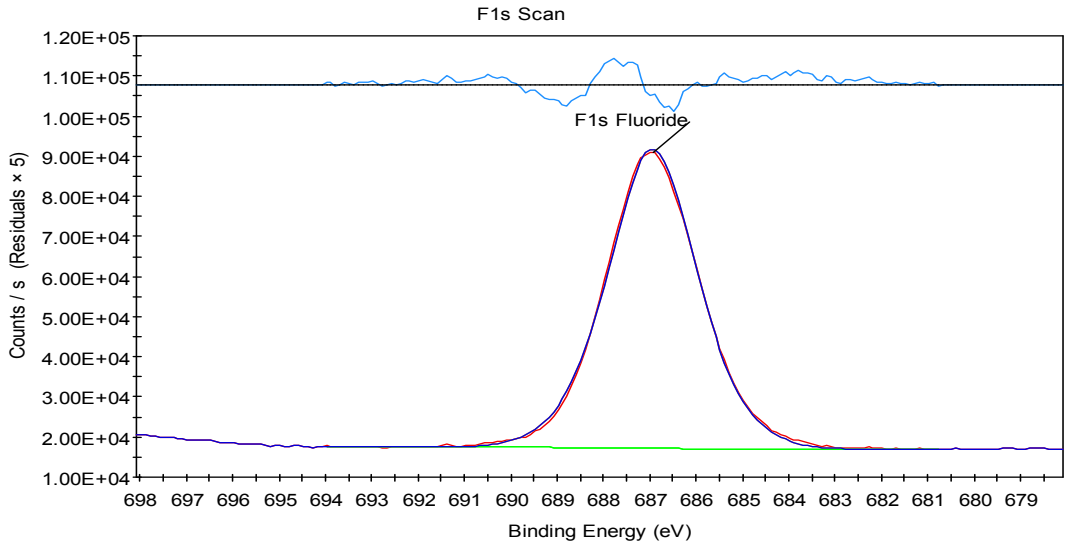

Figure S16. XPS full spectra of F1s.

Table S9. The spectra peaks and relative quantitative analysis for BBOFH.

Name	Peak of binding energy（BE）	Atomic %	Atomic % ratio	Peak Type
F1s Fluoride	686.94	23.81	5.95	Fitted
C1s C-C	284.8	28.63	7.16	Fitted
C1s C-O	286.79	2.22	0.56	Fitted
C1s C=O	288.83	1.07	0.27	Fitted
O1s C-O/C=O/OH/Borate	532.83	25.44	6.36	Fitted
B1s Borate	194.49	14.83	3.71	Fitted
Ba3d Oxide	781.57	4	1.00	Standard

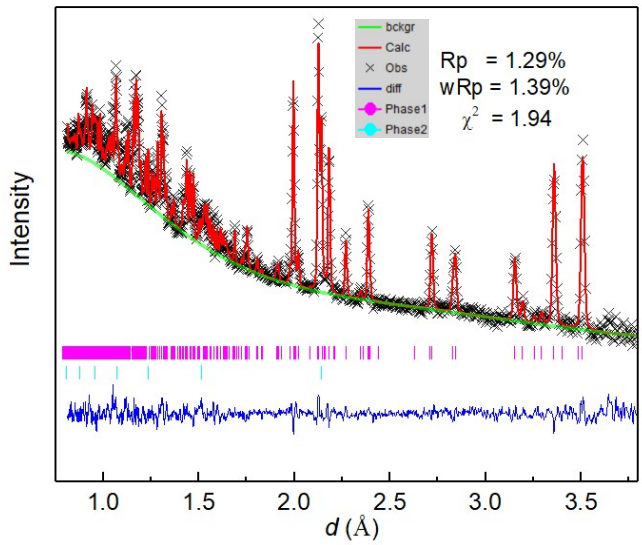

Figure S17. Neutron powder diffraction pattern of BBOFH (Sample 0.64 g) at room temperature. The crosses show the experimental intensities (I_{obs}), the upper solid line shows the calculated intensities (I_{calc}), and the lower solid line is the difference between the observed and calculated intensities (I_{obs}-I_{calc}). The vertical lines indicate the positions of the nuclear Bragg reflections of BBOFH (Phase 1) and vanadium holder (Phase 2) .

References

1. O. V. Dolomanov, L. J. Bourhis, R. J. Gildea, J. A. K. Howard, H. Puschmann, *J. Appl. Crystallogr.* **2009**, *42*, 339-341.
2. J. Clark Stewart, D. Segall Matthew, J. Pickard Chris, J. Hasnip Phil, I. J. Probert Matt, K. Refson, C. Payne Mike, *Z. Kristallogr.* **2005**, *220*, 567–570.
3. J. P. Perdew, K. Burke, M. Ernzerhof, *Phys. Rev. Lett.* **1996**, *77*, 3865-3868.
4. (a) W. L. Jia, J. Y. Fu, Z. Y. Cao, L. Wang, X. B. Chi, W. G. Gao, L. W. Wang, *J. Comput. Phys.* **2013**, *251*, 102-115; (b) W. L. Jia, Z. Y. Cao, L. Wang, J. Y. Fu, X. B. Chi, W. G. Gao, L. W. Wang, *Comput. Phys. Commun.* **2013**, *184*, 9-18.
5. N. E. Brese, M. O'Keeffe, *Acta Crystallogr.* **1991**, *B47*, 192-197.
6. G. Cakmak, J. Nuss, M. Jansen, *Z. Anorg. Allg. Chem.* **2009**, *635*, 631-636.
7. B. B. Zhang, G. Q. Shi, Z. H. Yang, F. F. Zhang, S. L. Pan, *Angew. Chem. Int. Ed.* **2017**, *56*, 3916-3919.
8. (a) T. Pilz, H. Nuss, M. Jansen, *J. Solid State Chem.* **2012**, *186*, 104-108; (b) T. Brauniger, T. Pilz, C. V. Chandran, M. Jansen, *J. Solid State Chem.* **2012**, *194*, 245-249.
9. Z. Z. Zhang, Y. Wang, B. B. Zhang, Z. H. Yang, S. L. Pan, *Angew. Chem. Int. Ed.* **2018**, *57*, 6577-6581.
10. G. Cakmak, T. Pilz, M. Jansen, *Z. Anorg. Allg. Chem.* **2012**, *638*, 1411-1415.
11. G. Q. Shi, Y. Wang, F. F. Zhang, B. B. Zhang, Z. H. Yang, X. L. Hou, S. L. Pan, K. R. Poeppelmeier, *J. Am. Chem. Soc.* **2017**, *139*, 10645-10648.
12. G. Q. Shi, F. F. Zhang, B. B. Zhang, D. W. Hou, X. L. Chen, Z. H. Yang, S. L. Pan, *Inorg. Chem.* **2016**, *56*, 344-350.
13. Y. Wang, B. B. Zhang, Z. H. Yang, S. L. Pan, *Angew. Chem. Int. Ed.* **2018**, *57*, 2150-2154.
14. M. Chrenková, V. Daněk, A. Silný, V. Kremenetsky, E. Polyakov, *J. Mol. Liq.* **2003**, *102*, 213-226.
15. G. P. Han, G. Q. Shi, Y. Wang, B. B. Zhang, S. J. Han, F. F. Zhang, Z. H. Yang, S. L. Pan, *Chem. - Eur. J.* **2018**, *24*, 4497-4502.
16. X. F. Wang, Y. Wang, B. B. Zhang, F. F. Zhang, Z. H. Yang, S. L. Pan, *Angew. Chem. Int. Ed.* **2017**, *56*, 14119-14123.
17. S. J. Han, B. B. Zhang, Z. H. Yang, S. L. Pan, *Chem. - Eur. J.* **2018**, *24*, 10022-10027.
18. D. Q. Jiang, Y. Wang, H. Li, Z. H. Yang, S. L. Pan, *Dalton Trans.* **2018**, *47*, 5157-5160.
19. C. C. Tang, X. X. Jiang, W. L. Yin, L. J. Liu, M. J. Xia, Q. Huang, G. M. Song, X. Y. Wang, Z. S. Lin, C. T. Chen, *Dalton Trans.* **2019**, *48*, 21-24.
20. S. J. Han, Y. Wang, B. B. Zhang, Z. H. Yang, S. L. Pan, *Inorg. Chem.* **2018**, *57*, 873-878.
21. D. Q. Jiang, G. P. Han, Y. Wang, H. Li, Z. H. Yang, S. L. Pan, *Inorg. Chem.* **2019**, *58*, 3596-3600.
22. M. Luo, F. Liang, Y. X. Song, D. Zhao, F. Xu, N. Ye, Z. S. Lin, *J. Am. Chem. Soc.* **2018**, *140*, 3884-3887.
23. Z. Z. Zhang, Y. Wang, B. B. Zhang, Z. H. Yang, S. L. Pan, *Inorg. Chem.* **2018**, *57*, 4820-4823.
24. M. Mutailipu, M. Zhang, B. B. Zhang, L. Y. Wang, Z. H. Yang, X. Zhou, S. L. Pan, *Angew. Chem. Int. Ed.* **2018**, *57*, 6095-6099.
25. S. G. Jantz, F. Pielnhofer, L. van Wüllen, R. Weihrich, M. J. Schäfer, H. A. Höppe, *Chem. - Eur. J.* **2018**, *24*, 443-450.
26. M. Luo, F. Liang, Y. X. Song, D. Zhao, N. Ye, Z. S. Lin, *J. Am. Chem. Soc.* **2018**, *140*, 6814-6817.
27. M. Mutailipu, M. Zhang, B. B. Zhang, Z. H. Yang, S. L. Pan, *Chem. Commun.* **2018**, *54*, 6308-6311.
28. R. H. Cong, Y. Wang, L. Kang, Z. Y. Zhou, Z. S. Lin, T. Yang, *Inorg. Chem. Front.* **2015**, *2*, 170-176.
29. C. M. Huang, F. F. Zhang, H. Li, Z. H. Yang, H. H. Yu, S. L. Pan, *Chem. - Eur. J.* **2019**, *25*, 6693-6697.
30. Z. Z. Zhang, Y. Wang, H. Li, Z. H. Yang, S. L. Pan, *Inorg. Chem. Front.* **2019**, *6*, 546-549.
31. A. C. Larson and R. B. Von Dreele, *General Structure Analysis System (GSAS). Report LAUR 86-748* (Los Alamos National Laboratory, Los Alamos, NM, 2000).